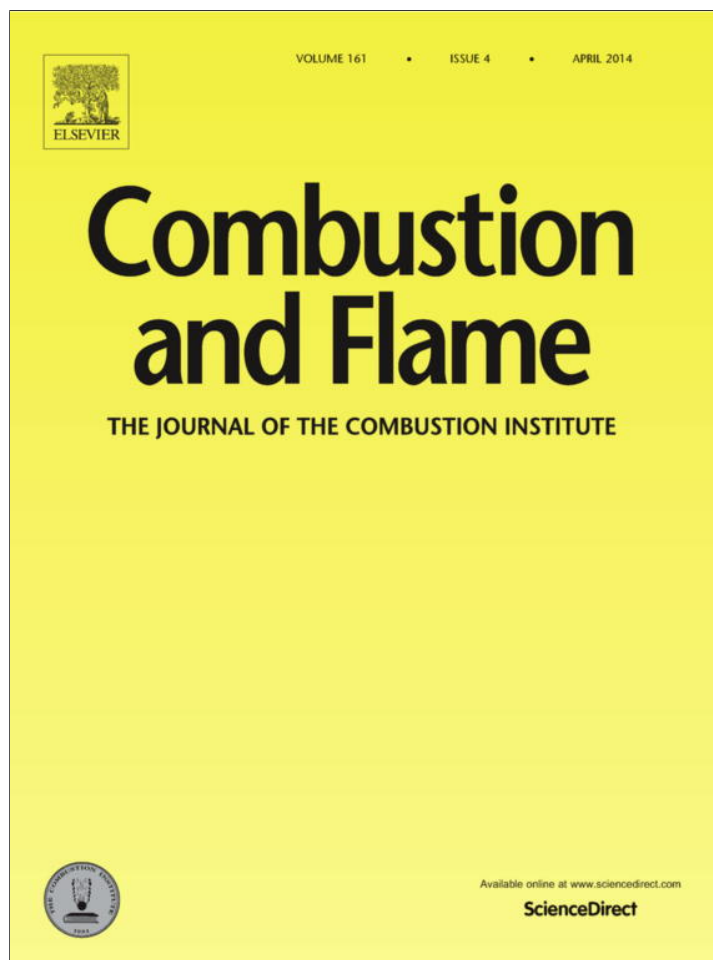


Provided for non-commercial research and education use.
Not for reproduction, distribution or commercial use.



This article appeared in a journal published by Elsevier. The attached copy is furnished to the author for internal non-commercial research and education use, including for instruction at the authors institution and sharing with colleagues.

Other uses, including reproduction and distribution, or selling or licensing copies, or posting to personal, institutional or third party websites are prohibited.

In most cases authors are permitted to post their version of the article (e.g. in Word or Tex form) to their personal website or institutional repository. Authors requiring further information regarding Elsevier's archiving and manuscript policies are encouraged to visit:

<http://www.elsevier.com/authorsrights>



Contents lists available at ScienceDirect

Combustion and Flame

journal homepage: www.elsevier.com/locate/combustflame

Stability enhancement of ozone-assisted laminar premixed Bunsen flames in nitrogen co-flow

Tran Manh Vu^a, Sang Hee Won^b, Timothy Ombrello^c, Min Suk Cha^{a,*}^a Clean Combustion Research Center, King Abdullah University of Science and Technology (KAUST), Thuwal 23955-6900, Saudi Arabia^b Department of Mechanical and Aerospace Engineering, Princeton University, Princeton, NJ 08544, United States^c Air Force Research Laboratory, Aerospace Systems Directorate, 1950 Fifth Street, Wright-Patterson AFB, OH 45433, United States

ARTICLE INFO

Article history:

Received 14 June 2013

Received in revised form 28 August 2013

Accepted 25 September 2013

Available online 17 October 2013

Keywords:

Ozone

Blowoff velocity

Plasma assisted combustion

Dielectric barrier discharge

ABSTRACT

Ozone (O₃) is known as one of the strongest oxidizers and therefore is widely used in many applications. Typically in the combustion field, a combination of non-thermal plasma and combustion systems have been studied focusing on the effects of ozone on flame propagation speeds and ignition characteristics. Here, we experimentally investigated the effects of ozone on blowoff of premixed methane/air and propane/air flames over a full range of equivalence ratios at room temperature and atmospheric pressure by using a co-flow burner and a dielectric barrier discharge. The results with ozone showed that a nozzle exit jet velocity at the moment of flame blowoff (blowoff velocity) significantly increased, and flammability limits for both fuel-lean and rich mixtures were also extended. Ozone had stronger effects of percent enhancement in the blowoff velocity for off-stoichiometric mixtures, while minimum enhancements could be observed around stoichiometric conditions for both fuels showing linear positive dependence on a tested range of ozone concentration up to 3810 ppm. Through chemical kinetic simulations, the experimentally observed trends of the enhancement in blowoff velocity were identified as a result of the modification of the laminar burning velocity. Two ozone decomposition pathways of O₃ + N₂ → O + O₂ + N₂ and O₃ + H → O₂ + OH were identified as the most controlling steps. These reactions, coupled with fuel consumption characteristics of each fuel determined the degree of promotion in laminar burning velocities, supporting experimental observations on blowoff velocities with ozone addition.

© 2013 The Combustion Institute. Published by Elsevier Inc. All rights reserved.

1. Introduction

Plasma-assisted combustion has been extensively studied over the last few decades and has shown promising effects on controlling or enhancing fundamental combustion phenomena, such as reducing ignition delay time [1–4], increasing flame propagation speed [5], enhancing flame stabilization [6–9], and reducing emissions [10,11]. Many feasibility tests of plasma-assisted combustion have been applied to systems using various types of plasmas ranging from thermal to non-thermal discharges, with care taken to consider how the discharge is coupled to the reactive system. Nevertheless, the coupling process can be complicated enough that it is difficult to quantify the enhancement mechanisms. These enhancement mechanisms can be summarized in three categories [3,12–17]; (1) thermal enhancement by joule heating, (2) chemical kinetic enhancement by active plasma species, and (3) manipulation of transport (diffusion and convection) properties through ionic wind effects.

Although thermal plasmas have shown the instantaneous impacts on enhancing ignition [18–20] and flame stabilization [21], more advanced semi-volumetric applications have been limited because of the inefficiency of plasma energy deposition caused by its intrinsic nature to be a localized discharge. In this regard, recent studies have devoted extensive efforts towards revealing the chemical kinetic enhancement mechanisms by implementing non-thermal plasmas, targeting its unique characteristics in generating active plasma species [9,14,22]. Non-thermal plasma has been known to be more effective than thermal plasma in producing active plasma species, such as active radicals, excited species, and ions/electrons, thus promoting the rate of chemical energy conversion, which consequently can significantly enhance combustion performance [16]. Furthermore, high electrical potentials of the order of kilovolts have been applied to combustion systems and it has been found that electric fields can also alter important transport properties in combustion processes. The changes of transport properties led to enhanced stability of non-premixed jet flames [17,23,24] and premixed flames [15,25], as well as increased flame propagation speeds for tribrachial flames [17,26] and outwardly propagating spherical premixed flames [27].

* Corresponding author. Address: 4700 KAUST, Thuwal 23955-6900, Saudi Arabia.

E-mail address: min.cha@kaust.edu.sa (M.S. Cha).

In terms of the methodology to couple the plasma energy into a reactive system non-thermally, there are three different strategic approaches; (1) pretreatment of reactants to reform/crack fuel molecules [28,29], or to supply plasma-generated chemically active species, (2) direct in situ plasma discharges on the reaction zone to activate electron induced chemistry (plasma chemistry) in a flame [11], and (3) after-treatment of combustion emission such as soot and NO_x [30]. Among the aforementioned approaches, the pretreatment of the oxidizer has been found to be very efficient in generating a more vigorous oxidizer, such as electronically excited oxygen, atomic oxygen, and ozone [12,13,31–33]. Furthermore, these oxidizer species can be selectively produced and/or isolated, thus enabling quantitative identification of the enhancement mechanisms [12,32,33].

By supplying oxygen to a non-thermal electrical discharge, oxygen atoms (O) can be released from O_2 by electron impact dissociation even at room temperature conditions, upon which they readily combined with molecular oxygen (O_2) to produce the stable species of ozone (O_3). Ozone is known as a powerful oxidant and has been widely investigated to increase the performance of combustion and to reduce emissions [31,34–36]. However, throughout the electrical discharge processes, other byproducts such as $\text{O}_2(v)$, $\text{O}(^1\text{D})$, $\text{O}(^1\text{S})$, $\text{O}_2(a^1\Delta_g)$, and $\text{O}_2(b^1\Sigma_g)$, have to be inevitably produced as well as other excited species, ions, and electrons [12,13]. Recently, Ombrello et al. [12,13] demonstrated that the effects of ozone, which has a relatively long lifetime compared to other plasma-produced species, could enhance the laminar burning velocity. The enhancement by ozone has been attributed to the fact that the decomposition of ozone early in the flame front provides O atoms, thus accelerating the fuel oxidation rate. Consequently, by adding several thousand parts per million (ppm) of ozone, it was found that the laminar burning velocities of hydrocarbon flames could be increased by a few percent [5,12,32,33].

Although the effects of ozone on laminar burning velocity of premixed flames have been reported, the effects of ozone on other flame phenomena, such as blowoff velocity and flammability limits, where the ozone impact might be magnified through the coupling between kinetics and hydrodynamics [12], remain unknown. In this regard, the objective of this study was to investigate the effect of ozone on the flame stability of premixed Bunsen flames. The blowoff velocities and flammability limits for fuel/air pre-mixtures were investigated in terms of ozone addition at atmospheric pressure and room temperature conditions. Two gaseous fuels, methane and propane, which have very different fuel fragmentation processes, were used to clarify the difference in chemical kinetic pathways by ozone addition. Detailed features of the enhancement of blowoff and the extension of flammability are discussed and supported by numerical simulations taking into account chemical kinetic pathways involved.

2. Experiment

The experimental apparatus consisted of a co-flow burner, flow controllers, an ozone generator, an ozone monitor, and a laser-induced fluorescence system for OH radicals, as schematically shown in Fig. 1. The co-flow burner had a central nozzle made of stainless steel with its inner and outer diameters of 7.53 mm and 9.54 mm, respectively. To ensure a fully developed parabolic velocity profile at the nozzle exit up to the maximum velocity of the present experiment, well known laminar flow correlations for an entrance length for the fully developed velocity profile, (length of nozzle)/(inner diameter of nozzle) $\sim 0.06 \text{ Re}$ [37], was considered. By using a 470 mm-length tube, 60 times the nozzle diameter, a fully developed parabolic velocity profiles at the nozzle exit was assured for all flow conditions (Reynolds number < 1000 , thus laminar

regime) in this study. To obtain a uniform flow distribution throughout the co-flow section, a layer of glass beads was packed under a ceramic honeycomb. A nitrogen (N_2) co-flow was used to isolate premixed flames from secondary diffusion flames formed with ambient air at fuel rich conditions, and its flow velocity was fixed at 10.2 cm/s for all test conditions. Mass flow controllers (Brooks Instrument, 5850E) calibrated by a dry-test gas meter (Bios, Definer 220M) were used to control the flow rates of the gases. Methane (CH_4 , 99.95%) and propane (C_3H_8 , 99.5%) were selected as the fuels, and oxygen (O_2 , 99.9995%) and nitrogen (N_2 , 99.9999%) were separately supplied keeping their composition as that of air.

A coaxial type dielectric barrier discharge (DBD) reactor was employed as the ozone generator. A quartz tube was used as a dielectric material having an outer diameter of 30 mm, an inner diameter of 27 mm, and a length of 300 mm. Stainless steel mesh wrapped around the quartz tube with 200 mm in length served as a ground electrode. At the center of the quartz tube, a stainless steel rod with an outer diameter of 25 mm was used as a high voltage electrode; creating a gap between the center electrode and the quartz tube of 1 mm. A power amplifier (Trek, 40/15-H-CE), which could supply voltage and current up to 40 kV and 15 mA, respectively, in conjunction with a function generator (Tektronix, AFG3021B) was used to generate high voltage AC with an arbitrary frequency and energize the ozone generator. The operating frequency and the applied voltage were changed to adjust ozone concentration in the oxidizer stream. It was found that the conditions of $V = 7.28 \text{ kV}$ in rms value and $f = 700 \text{ Hz}$ provided a maximum concentration of ozone of 3810 ppm. High-purity oxygen was flowed into the ozone generator to achieve higher yields of ozone without undesired plasma byproducts, such as NO_x [12]. Then, as shown in Fig. 1, the ozone containing oxygen stream was mixed with nitrogen to match the air composition (21% O_2 and 79% N_2 by volume). The ozone concentration in the O_2 - N_2 mixture (synthetic air) was measured with a UV ozone monitor (Ebara Jitsugyo, EG-3000). Finally, the ozone containing synthetic air stream was mixed with fuel to form the target equivalence ratio of the fuel/air mixture.

In order to ensure that the ozone measured in the UV ozone monitor was in fact what was entering the flame, a parametric study was performed. The DBD discharge produces many other species besides ozone, such as O, $\text{O}(^1\text{D})$, and $\text{O}_2(a^1\Delta_g)$. However, since the lifetime of these metastable oxygen species is extremely short at atmospheric pressure [12], the only long lived species is ozone. Therefore, to confirm experimentally that the ozone concentration was constant, different lengths of tubing were tested to vary the flow residence time for the range of conditions used in the experiments. The lack of change in the measured ozone concentration with the different length tubes verified that ozone was the only plasma-produced species present at the ozone monitor. Furthermore, changing the length of tubing between the fuel mixing location and the burner resulted in no changes to the flame. The result confirmed there was no reaction of ozone with the fuels, which is reasonable because ozone reactions with alkanes are very slow at low temperature (295 K) [12,38].

The most important parameter investigated was the blowoff limit of the premixed flames along with the equivalence ratios, ϕ , of the mixtures. Experimentally, to determine a critical nozzle exit velocity at the moment of flame blowoff, a nozzle exit velocity, u_{jet} , needed to be varied while maintaining a given equivalence ratio. Since it was difficult to maintain the same concentration of ozone when u_{jet} was varied, a bypass system was designed into the experiment. First, the flow rate of oxygen was fixed at 2 l/min, which could accommodate the highest flow rate condition used in the experiments. By fixing the applied voltage and frequency to the ozone generator, the production rate of ozone could be locked,

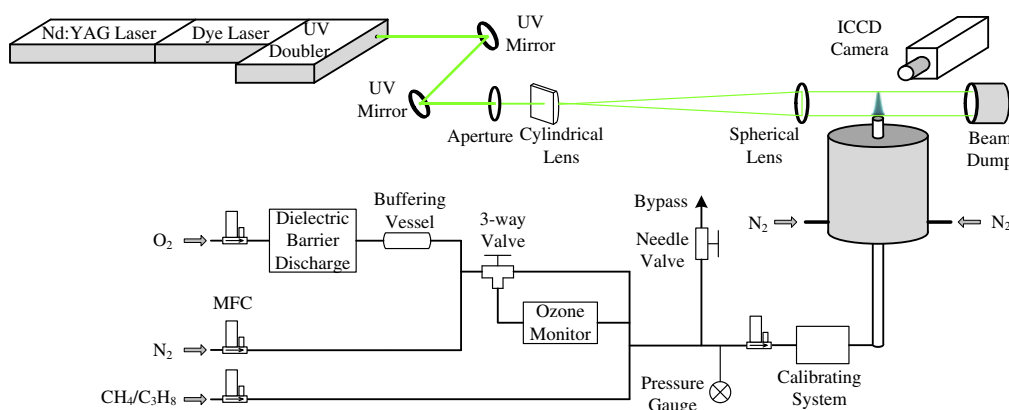


Fig. 1. Schematic of experimental setup.

and a constant ozone concentration could be guaranteed by mixing the corresponding amount of nitrogen. Then, the fuel flow rate was determined based on the oxygen flow rate (fixed at 2 l/min) for a target equivalence ratio. Finally, the jet velocity at the nozzle exit was adjusted with the downstream mass flow controller (MFC) by venting the remainder of a mixture, as shown in Fig. 1. Note that the most downstream MFC was pre-calibrated for all equivalence ratios used in the experiments with the dry test gas meter.

However, there was an additional difficulty to ensure electrical discharge characteristics inside the ozone generator because the discharge characteristics and consequent production of ozone were sensitive to pressure. To avoid such a problem in fluctuating ozone concentration, a needle valve and a pressure gauge were installed in the vented line and in front of the most downstream MFC to maintain a constant pressure inside the ozone generator. The pressure inside the ozone generator was maintained at 1.2 bar by monitoring the pressure gauge (Keller, LEO3). A digital camera (Nikon, N700) equipped with a Micro-Nikkor 105 mm f 2.8 lens was used to capture direct images of the flames.

To visualize the change in flame structure by O_3 addition, a laser-induced fluorescence (LIF) technique for OH radicals was adopted. The laser setup consisted of a Nd:YAG pulsed laser (Continuum, Powerlite DLS 9010), a tunable dye laser (Continuum, ND6000) with rhodamine 590 (Exciton), and a frequency doubling unit (Continuum, UVT-3). The wavelength of the UV output was tuned according to the $Q_1(6)$ transition of the $A^2\Sigma^+ - X^2\Pi(1, 0)$ band for the OH radical at 282.96 nm. The laser beam was expanded to a 5 cm-height sheet ($\sim 250 \mu\text{m}$ thickness) by an $f = 150$ mm cylindrical lens and an $f = 1000$ mm spherical lens. An intensified charge-coupled device (ICCD, Princeton Instrument, PI-MAX3: 1024i), together with a UV Nikkor 105 mm f 4.5 lens, was used to capture the OH fluorescence signal with a set of WG305 and UG11 filters.

3. Results and discussion

3.1. Flames observation

Figure 2 shows the direct photographs of the nozzle-attached premixed Bunsen flames at three equivalence ratios ($\phi = 0.8, 1.0,$ and 1.3) for both methane (a) and propane (b), just prior to blow-off. To demonstrate the changes of flame structure by ozone addition, the flame images with ozone addition were taken at the same u_{jet} as the flames without ozone. The settings of the camera, such as shutter speed and ISO, were also kept constant for the direct comparison among captured flames. Direct photographs in Fig. 2 show the typical conical shape of premixed Bunsen flames, demon-

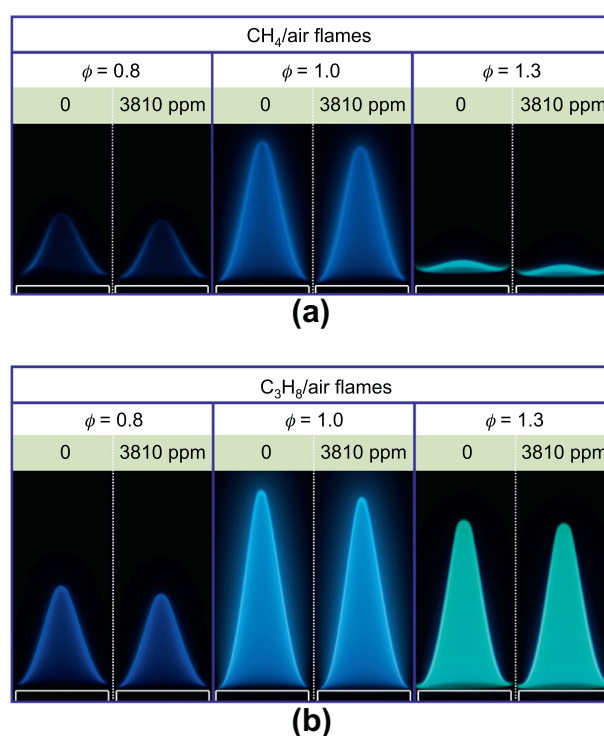


Fig. 2. Direct photographs of flames without and with O_3 of 3810 ppm addition; (a) methane/air flames with $u_{\text{jet}} = 49.1, 124.4,$ and 28.2 cm/s for $\phi = 0.8, 1.0,$ and $1.3,$ respectively, (b) propane/air flames with $u_{\text{jet}} = 76.9, 183.7,$ and 117.7 cm/s for $\phi = 0.8, 1.0,$ and $1.3,$ respectively. Note that white solid line indicates the nozzle.

strating the changing color¹ of flame luminosity from blue at the lean condition to greenish blue at the rich condition [39]. Regardless of fuel and equivalence ratio, we observed that the flame heights at the tip of the flames decreased with the addition of ozone, e.g. for propane/air flame at $\phi = 0.8,$ the flame height was measured at 9.85 mm but decreased to 9.2 mm with the addition of 3810 ppm of ozone. In a premixed Bunsen flame, the cone angle is predominantly determined by the balance between the laminar burning velocity and the local flow velocity [33]. As a consequence of the change in either one of the velocities, the cone angle readjusts and results in flame height modification. Thus, the reductions of the flame heights by adding ozone strongly indicated the enhancement

¹ For interpretation of color in Fig. 2, the reader is referred to the web version of this article.

of laminar burning velocity because u_{jet} was maintained at a constant value.

It is worth mentioning that the addition of ozone reduced not only the flame height but also the height of the flame base from the nozzle rim (standoff distance) for all conditions in Fig. 2. The noticeable reduction in the standoff distance was observed particularly at the rich conditions ($\phi = 1.3$) of methane flames. Although the detailed mechanism for flame base anchoring on the nozzle rim encompasses the complicated flame dynamics associated with near nozzle flow-field, flame stretch, heat transfer with the nozzle, chemical kinetic potential of fuel, mixing with co-flow gas, etc., the reduction in the flame standoff distance also implied the enhancement of laminar burning velocity through ozone addition [12,32,33]. When comparing the two fuels, propane/air flames were found to be more stable than methane/air flames especially at the rich condition, showing the higher flame height prior to blowoff as a result of higher u_{jet} . This was attributed to the fact that propane/air flames have higher extinction limits than methane/air flames [40] as well as higher laminar burning velocity at rich conditions [41]. Noting that the nozzle exit velocity prior to blowoff for the propane/air flame shown in Fig. 2(b), 117.7 cm/s, was a factor of 4 higher than that of the methane/air flame, 28.2 cm/s at $\phi = 1.3$, it is of interest to point out that the extinction stretch rate of propane/air premixed flames is also a factor of 4 higher than that of methane/air premixed flames at the same equivalence ratio, $\phi = 1.3$ [40].

To further investigate the detailed influence of ozone on flame structure, cross-sectional images of OH radicals using the planar laser induced fluorescence (PLIF) technique are shown in Fig. 3. Each OH PLIF image was the result of an average of 20 instantaneous images, normalized with the laser beam profile after subtracting a background signal. The equivalence ratios and u_{jet} were selected to be the same as the direct photographs shown in Fig. 2. The left half of each image represents the normal premixed flame without ozone addition, while the right half of the image shows the OH distribution with ozone addition. The LIF intensities were consistently normalized by the maximum LIF intensity of the flame without ozone addition for each comparison, thus the direct comparison of LIF intensity represented the change of OH concentration by ozone addition for each equivalence ratio. In reality, the concentration of OH (OH LIF intensity) in the fuel-rich flame was much lower than the other mixtures. In terms of peak OH concentration, there were no significant changes between the flame with and without ozone addition. However, the spatial distributions of OH clearly demonstrated the change of flame heights and standoff distance, indicating the enhancement of laminar burning velocity by ozone addition as discussed above with regard to the direct photographs.

The blowoff of premixed Bunsen flames has been understood to occur when the burning velocity at the leading edge, here the flame base near the nozzle rim, becomes lower than the local flow velocity. Also, at the same time the gradient of the local laminar burning velocity must be greater than that of the local flow velocity along

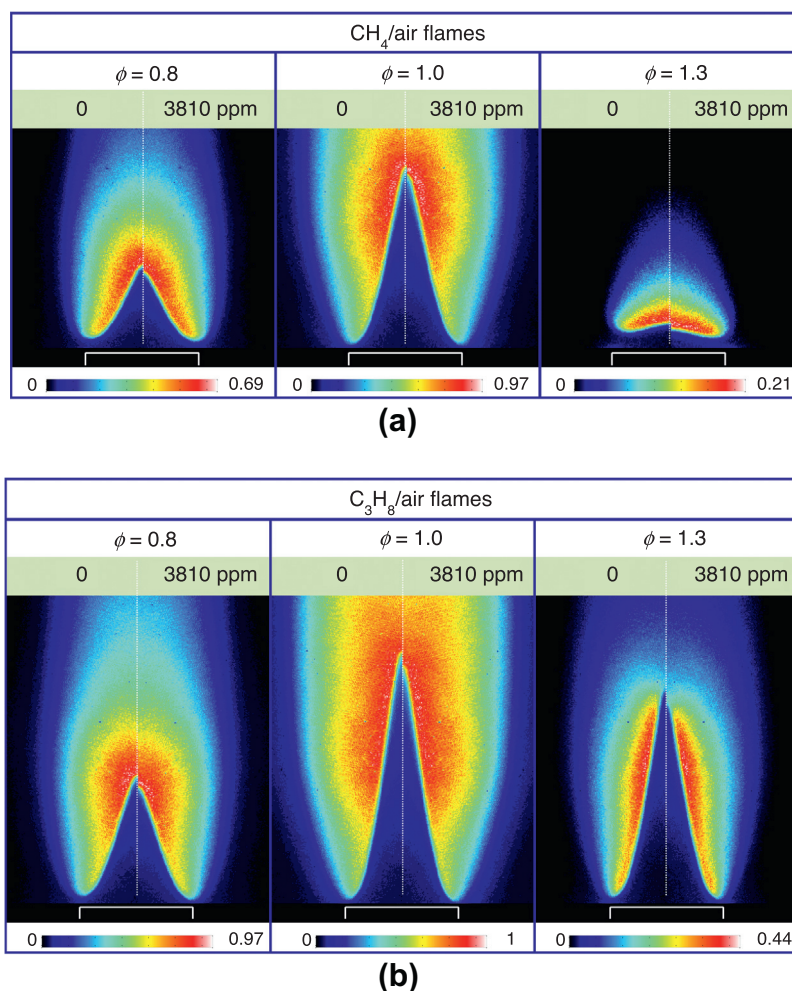


Fig. 3. Qualitative PLIF images of OH distribution without and with O₃ of 3810 ppm addition; (a) methane/air flames with $u_{jet} = 49.1, 124.4,$ and 28.2 cm/s for $\phi = 0.8, 1.0,$ and 1.3 , respectively, (b) propane/air flames with $u_{jet} = 76.9, 183.7,$ and 117.7 cm/s for $\phi = 0.8, 1.0,$ and 1.3 , respectively. Note that white solid line indicates the nozzle, and the intensities of images were normalized with that of propane/air flame of $\phi = 1.0$ without ozone.

with the direction of propagation at the flame anchoring position [42]. However, a recirculating flow might form near a finitely thick nozzle rim, or even worse the burning velocity at the flame base can undergo hydro-thermal effects, such as stretch of the flame surface, heat loss to the nozzle rim, radical termination or quenching at the nozzle surface, dilution with ambient gas, and so forth. Thus the blowoff cannot be fully explained simply by using the laminar burning velocity at a given equivalence ratio. Nevertheless, the PLIF images show that the OH concentration at the flame base decreased compared to other areas in the flame zones, regardless of the flow conditions in Fig. 3. Considering that the OH concentration is directly related with the heat release rate [43–45], the results of OH PLIF at the flame base indicated the weakened reactivity and thus decreased burning velocity prior to the blowoff due to the aforementioned hydro-thermal effects. It is also noteworthy that the flame tip of the propane/air mixture at $\phi = 1.3$ in Fig. 3(b) exhibited a relatively weak OH signal, whereas other flames showed the most intensified OH concentrations. When the Lewis number became substantially lower than unity as for rich propane/air premixed flames, the negative stretch at the flame tip decreased the flame strength.

Distinctive behaviors of flame structure caused by low Lewis number for the case of rich premixed propane flames were further observed by increasing the equivalence ratio. Similar to other relevant studies [46], we observed polyhedral flames and spinning partially lifted flames for rich propane/air mixtures. In Fig. 4, the direct photos of the rich propane/air flames are shown together with the images for the influenced flames by adding ozone. For $\phi = 1.4$, a five-sided polyhedral flame was observed without ozone addition, which was caused by a thermo-diffusive instability for sufficiently low Lewis numbers [42]. However, by adding O_3 to the same mixture of $\phi = 1.4$, besides the reduction in the flame height, the sharp ridges between the planes appeared to be smoothed. Further increasing the equivalence ratio to $\phi = 1.5$ (this was the rich extinction limit of the propane/air flame without O_3 addition), as shown in Fig. 4(c) a spinning X-flame could be observed (the flame looks like an 'X' when using a long exposure for the photograph). This was a result of the rotation of a partially attached (or lifted) flame along the circumference of the nozzle rim. On the other hand as shown in Fig. 4(d), when 3810 ppm of ozone was added, the spinning X-flame turned back to a fully nozzle attached conical flame. Note that the blurred image in Fig. 4(d) is a result of an intermittent partial detachment of the conical flame with a long exposure time of the camera. For further increasing ϕ , an extension of the rich flammability limit to $\phi = 1.55$ with 3810 ppm of ozone was found, where only a spinning flame could be observed as shown in Fig. 4(e). Though the results showed that the instability could be explained qualitatively based on the preferential diffusion and the hydrodynamic response of the flames, the

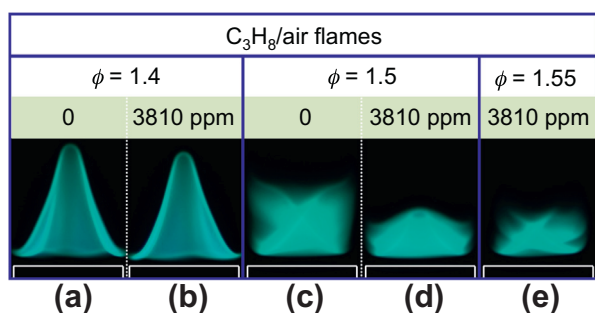


Fig. 4. Direct photographs of propane/air flames without and with O_3 of 3810 ppm addition at very rich and rich limit conditions; $u_{jet} = 64.9$ cm/s for (a, b) with $\phi = 1.4$, 29.8 cm/s for (c, d) with $\phi = 1.5$, and 21.9 cm/s for (e) with $\phi = 1.55$. Note that white solid line indicates the nozzle.

explanation on the mitigation of the flame instability by adding ozone requires a more detailed understanding of the chemical kinetics involved.

3.2. Blowoff characteristics

As previously mentioned, the blowoff characteristics are mainly affected by the laminar burning velocity, the local flow velocity, and their gradients along with the local direction of the flame propagation. However, the relationship is complicated due to the significant coupling that might occur. The laminar burning velocity, as an example, is a function of flame temperature and mixture composition. Near the nozzle rim where the flame base anchors, the flame temperature tends to decrease since there is heat loss to the nozzle and dilution with entrained ambient gas. A decrease in flame temperature leads to a negative effect on the local laminar burning velocity. On the contrary, the heated nozzle would be a source of heat to the unburned mixture, thus the reactant having elevated temperature would have a positive impact on the local laminar burning velocity. In this regard, when a blowoff velocity, $u_{b,o}$, was measured by increasing the flow rate of a mixture, the experimental results were significantly affected by the rate of time required to increase the flow rate, resulting in inconsistent determination of the blowoff velocity. Thus, to measure the blowoff velocity in a quasi-steady manner, instead of using an *increasing flow rate scheme* to find the critical blowoff conditions, we employed a *decreasing flow rate scheme*. The experiment was performed by initially setting u_{jet} to be higher than what is needed for flame blowoff. Then, the flow rate was continuously decreased until a flame could be ignited and stabilized near the nozzle exit. By doing this, it was assumed that the upstream gas heating from the heated nozzle could be ignored, thus the thermal boundary condition of the nozzle was fixed at room temperature.

The blowoff velocities together with the lean and rich flammability limits of the methane/air and the propane/air flames at atmospheric pressure and room temperature (~ 295 K) were experimentally determined and the stability domain of methane and propane flames are plotted in Fig. 5(a) and (b), respectively. The results showed that the blowoff velocities had similar trends with that of the laminar burning velocities for the corresponding mixtures, showing peaks at $\phi = 1.0$ – 1.1 and around $\phi = 1.1$ for the methane/air and the propane/air premixed flames, respectively [41]. A significant increase in blowoff velocities was found, and both the lean and rich flammability limits were extended for all tested fuel/air mixtures by adding 3810 ppm of ozone. The ranges of experimental uncertainty were also plotted with error bars for each of the tested conditions. We considered errors caused by the mass flow controllers, the ozone monitor, and experimental repeatability. Maximum uncertainties in $u_{b,o}$ were found to be 4.6% for both fuel/air mixtures with ozone in Fig. 5.

To quantify the effects of ozone addition on the blowoff velocities, the percent enhancements of $u_{b,o}$ based on $u_{b,o}$ of the corresponding mixtures without ozone, $(u_{b,o}|_{ozone} - u_{b,o}|_{normal}) / u_{b,o}|_{normal} \times 100$, are plotted in Fig. 6. The plot shows minimum enhancements at $\phi = 1.0$ – 1.1 and $\phi = 1.1$ for the methane/air and the propane/air flames, respectively, and the enhancement became magnified as the mixture equivalence ratio went either leaner or richer. By comparing the stoichiometric mixtures of the tested fuels, it was found that the propane/air mixture showed more noticeable enhancement in blowoff velocity over the methane/air flame. However, as the mixtures became richer, the methane/air mixture demonstrated a rapid increase in the percent enhancement of the blowoff velocity, showing higher enhancement than the propane/air mixtures for $\phi > 1.2$.

The sensitivity of the enhancements of blowoff velocity as a function of ozone concentration was also experimentally

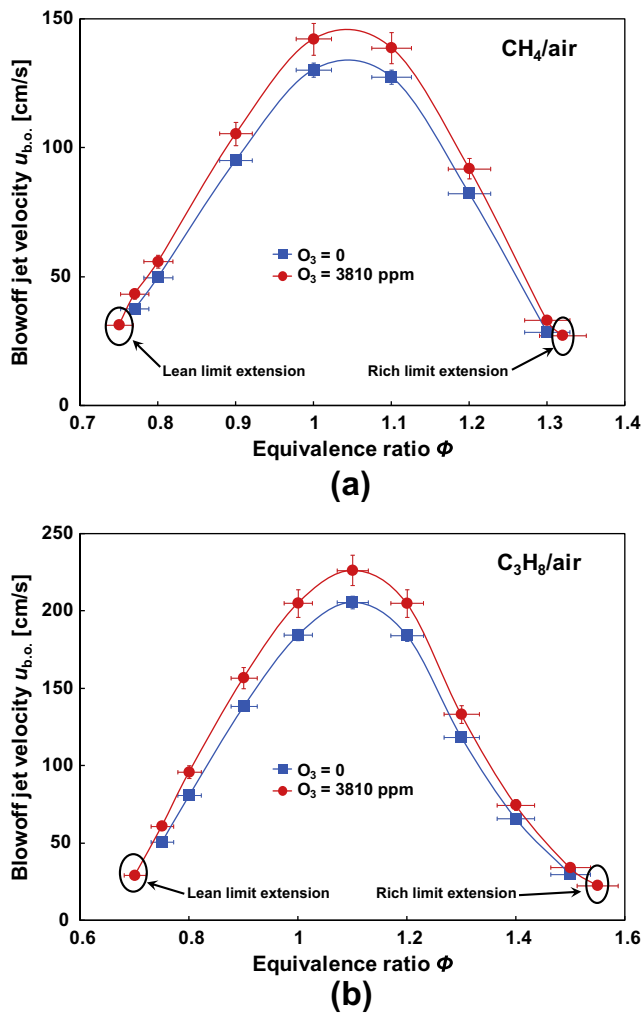


Fig. 5. Comparison of blowoff velocities without and with O₃ of 3810 ppm addition; (a) methane/air flames, (b) propane/air flames for various equivalence ratios.

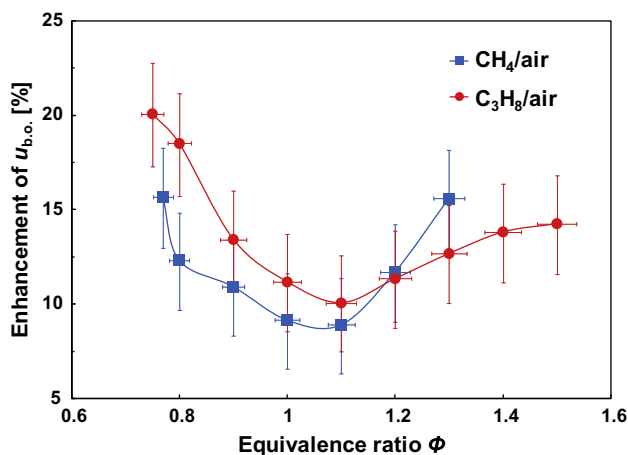


Fig. 6. Percent enhancement of blowoff velocities with 3810 ppm of O₃ addition for methane/air and propane/air flames as a function of equivalence ratio.

investigated at three equivalence ratios, $\phi = 0.8, 1.0,$ and $1.3,$ and the results are plotted in Fig. 7. The percent enhancement in blow-off velocity increased linearly with the tested range of ozone concentration for both fuels. The results were consistent with a previous study that examined the effect of ozone on stoichiometric

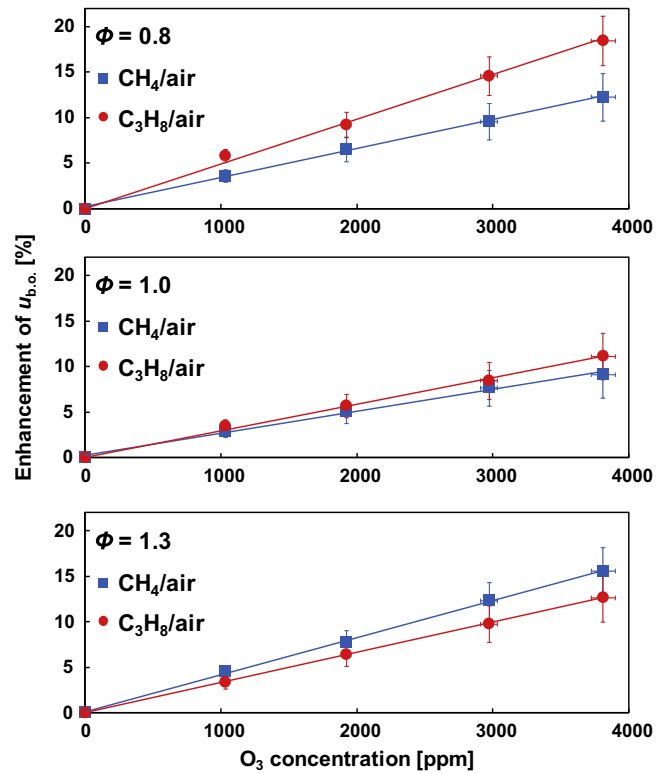


Fig. 7. Comparison of percent enhancement of blowoff velocities between methane/air and propane/air flames as a function of O₃ concentration.

propane/air [12] showing the linear increase of laminar burning velocity with ozone concentration. Motivated by the fact that the blowoff velocity was linearly correlated with ozone concentration across a range of equivalence ratios and that it followed the enhancement of laminar burning velocity, the chemical kinetic impact of ozone addition for both flames is discussed further in the following section, with focus primarily on the change of laminar burning velocity as a surrogate for the enhancement of the blowoff velocity by ozone addition.

3.3. Numerical simulations

From the chemical kinetic point of view, one might assume that ozone addition would be more effective on premixed methane/air flames than propane/air flames in terms of enhancing laminar burning velocity based on two previously addressed facts; (1) the addition of ozone resulted in earlier deposition of atomic oxygen through thermal decomposition reaction, $O_3 + N_2 \rightarrow O + O_2 + N_2$, in the preheat zone [12], and (2) premixed methane/air flames have a weaker radical pool than premixed propane/air flames [41]. Therefore, the addition of atomic oxygen may play a significant role on the radical pool population in premixed methane/air flames. However, as discussed above, the experimental results for blowoff velocities with ozone addition exhibited contradictory trends. Blowoff velocities of the premixed propane/air flames were more effectively enhanced for lean and near stoichiometric mixtures compared to the premixed methane/air flames, while the enhancement in $u_{b.o.}$ of the premixed methane/air flames prevailed over the propane/air mixture only for the fuel rich condition of $\phi > 1.2$. To clarify the discrepancy and provide supporting evidence to the experimental results, numerical simulations were performed using the PREMIX code of the CHEMKIN-PRO package [47]. Freely propagating laminar flame calculations were reasonable because the most important parameter affecting the blowoff velocity is

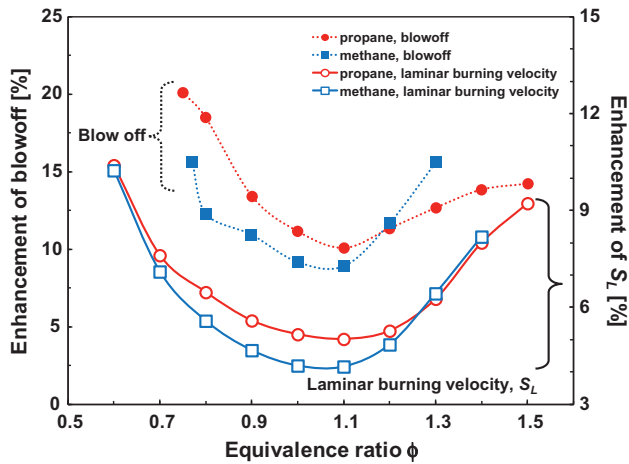


Fig. 8. Percent enhancement of calculated laminar burning velocity compared to the blowoff velocities with 3810 ppm of O₃ addition for methane/air and propane/air flames as a function of equivalence ratio.

the laminar burning velocity. The USC Mech II chemical kinetic mechanism was used for all simulations [48]. An O₃ sub-mechanism originally defined in Ref. [12] and updated with some of the reactions in the two recent studies on O₃ enhancement of CH₄ flames [32,33] was used. In Fig. 8, a comparison of the calculated enhancement in the laminar burning velocity with the enhancement in the blowoff velocity from Fig. 6 is shown. Similar to the blowoff experiments, ozone enhanced the laminar burning velocities for the propane/air mixtures more than the methane/air mixtures except for rich conditions above approximately $\phi = 1.2$.

In order to understand the role of ozone on the laminar burning velocity, the major consumption pathways of O₃ were analyzed for $\phi = 0.6, 1.0,$ and 1.4 respectively representing lean, stoichiometric, and rich conditions for both mixtures. As shown in Fig. 9, in the temperature range of 500–700 K, O₃ began to decompose through two major pathways of (~95% of total O₃ consumption fluxes)

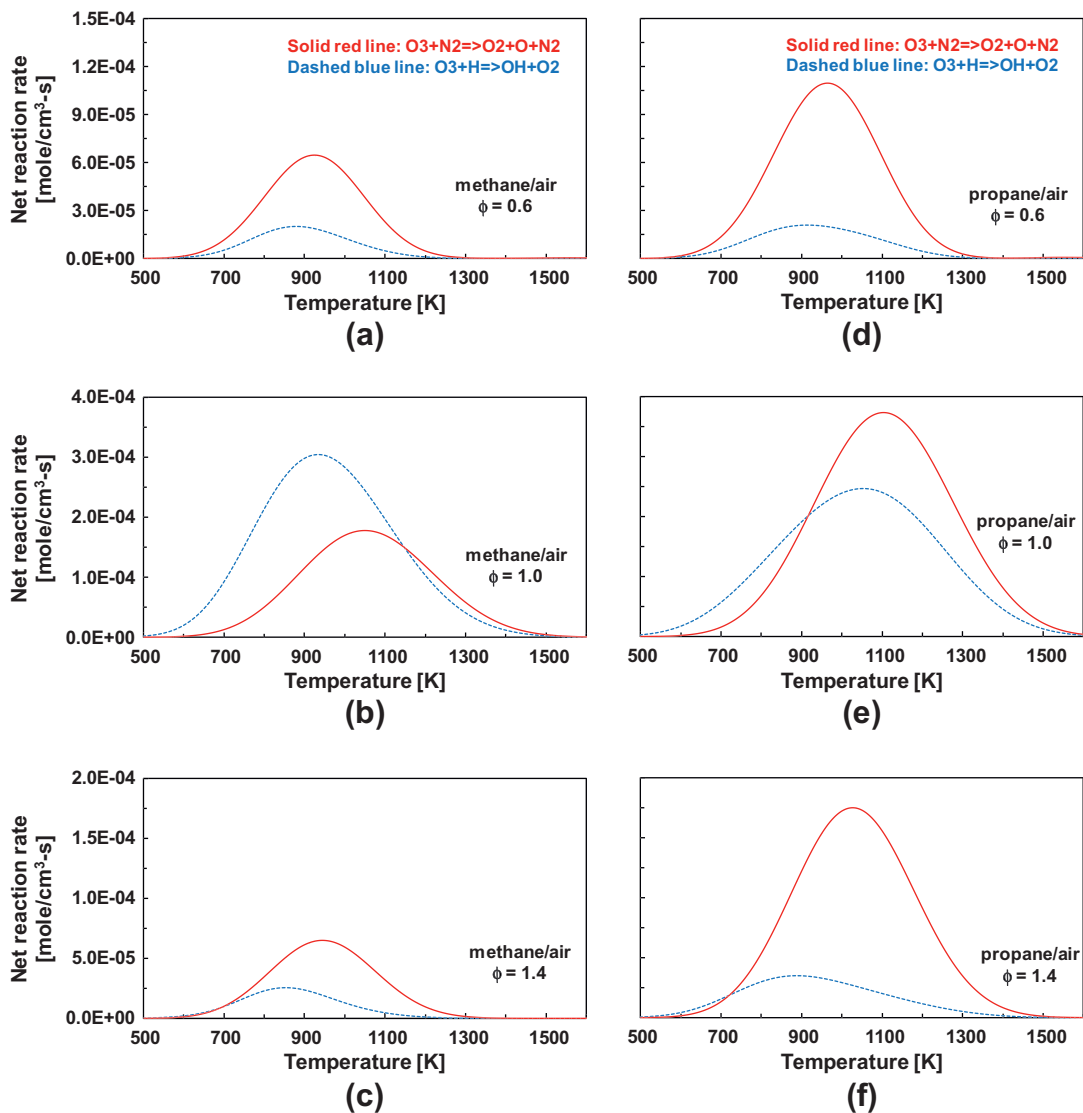


Fig. 9. Major consumption pathways of O₃ as a function of temperature through the flame at $\phi = 0.6, 1.0$ and 1.4 with 3810 ppm of O₃ addition for methane/air and propane/air flames.

with clear differences being seen for both fuels between stoichiometric and off-stoichiometric equivalence ratios. Here, the direct reactions of ozone to the hydrocarbon molecules were not considered in O_3 sub-mechanism, since their reaction rates were several orders of magnitude slower than the O_3 decomposition reactions, (R.1) and (R.2) as discussed in [12]. Indeed, the reaction of $O_3 + CH_3 \rightarrow CH_3O + O_2$ was included in those calculations, since CH_3 is a major intermediate species of methane oxidation, however its contribution to O_3 decomposition was found to be less than 1% for all tested conditions and also negligible from the sensitivity analysis, confirming the negligible contribution of the direct reactions of ozone to other hydrocarbon molecules.

Typically for both methane/air and propane/air flames at off-stoichiometric (lean and rich) conditions, ozone decomposition mainly occurred by (R.1), while (R.2) played a considerable role for stoichiometric conditions. The reaction (R.1) can be considered as a chain initiation reaction to produce active atomic O, whereas the reaction (R.2) is a chain propagation reaction, which converts H atom to OH radical. Thus, it was speculated that reaction (R.1) could be more beneficial to enhance the laminar burning velocity. To validate this hypothesis, a sensitivity analysis, perturbing a reaction rate and monitoring the subsequent change of the laminar

burning velocity, was also conducted for both fuels by varying the equivalence ratio. The results revealed that the logarithmic sensitivity coefficient of reaction (R.1) varied from 0.0024 to 0.0042 for both fuels while for reaction (R.2) showed negative values from -0.002 to -0.0035 , supporting the hypothesis above. Therefore, due to the effective atomic oxygen deposition via reaction (R.1) for the off-stoichiometric mixtures, a more pronounced enhancement in the blowoff velocity compared to the stoichiometric mixtures could be obtained for both mixtures. In addition, reaction (R.1) was still the dominant pathway for ozone reaction for the stoichiometric propane/air mixture (Fig. 9(e)), while reaction (R.2) became stronger than (R.1) for the stoichiometric methane/air mixture (Fig. 9(b)). In this regard, it could be concluded that the stoichiometric methane/air mixture would show the least enhanced laminar burning velocity, which agrees well with the experimental results of the blowoff velocity.

To cross validate the aforementioned discussion, the fuel consumption reactions are plotted in Fig. 10. Since more than 95% of the fuel consumption took place through H abstraction reactions, three H abstraction pathways were considered, which were fuel + H, fuel + O, and fuel + OH. For the stoichiometric methane/air flame in Fig. 10(b), the decomposition of ozone via reaction

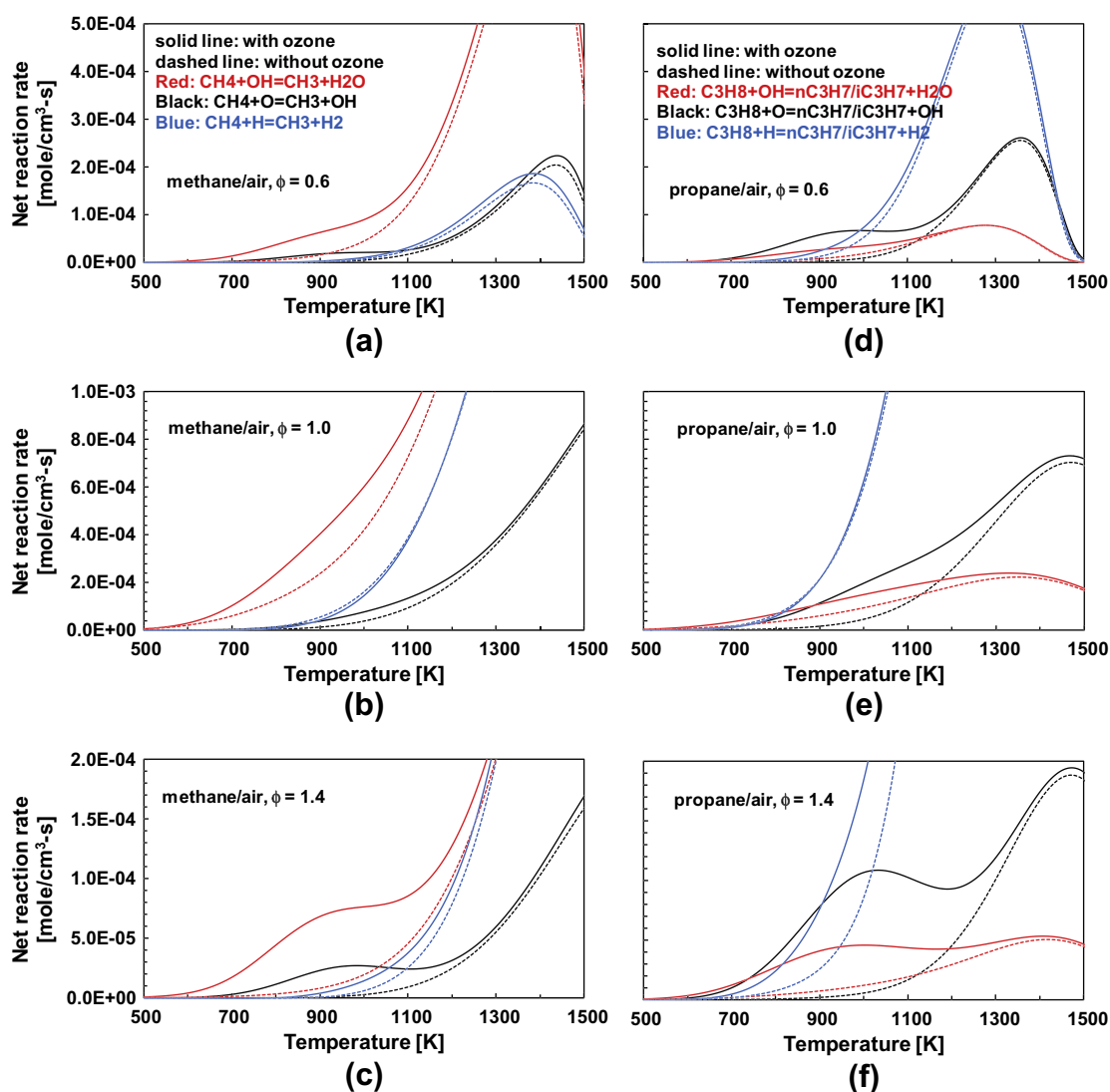


Fig. 10. H abstraction reaction rates of fuel oxidation pathways as a function of temperature for both methane/air (a–c) and propane/air (d–f) premixed flames at $\phi = 0.6, 1.0,$ and $1.4;$ with 3810 ppm of O_3 addition (solid lines) and without O_3 addition (dashed lines).

(R.2) provided OH early in the reaction zone (Fig. 9(b)), thus promoting the reaction of $\text{CH}_4 + \text{OH}$. Later in the reaction zone, from 700 K and higher temperatures, O was supplied through reaction (R.1) (Fig. 9(b)), resulting in a relatively small increase in the $\text{CH}_4 + \text{O}$ reaction. Note that this temperature dependence was strongly dictated by the decomposition of ozone shown in Fig. 9(b). On the other hand, for the stoichiometric propane/air flame shown in Fig. 10(e), as expected by the ozone decomposition in Fig. 9(e), stronger enhancement of the $\text{C}_3\text{H}_8 + \text{O}$ reaction was found when compared to $\text{C}_3\text{H}_8 + \text{OH}$.

Unlike the H abstraction reaction by OH (fuel + OH) that substituted active radicals for heat formation by producing stable H_2O , the H abstraction reaction by O (fuel + O) provided another active OH radical, which could be recycled back to the fuel decomposition pathway. Through this process, the stronger H abstraction reaction by O in the stoichiometric propane/air mixture led to superior enhancement in the laminar burning velocity compared to the stoichiometric methane/air mixture. This radical recycling and coupling impact through H abstraction reactions by O is demonstrated further for lean ($\phi = 0.6$) and rich ($\phi = 1.4$) mixtures shown in Fig. 10 (a and c) for methane and (d and f) for propane. As described above, the deposition of O via reaction (R.1) increased the reaction rate of $\text{CH}_4 + \text{O}$ or $\text{C}_3\text{H}_8 + \text{O}$, and in turn, the reactions of $\text{CH}_4 + \text{OH}$ or $\text{C}_3\text{H}_8 + \text{OH}$ were promoted.

In summary, the numerical analysis revealed that the enhancement of laminar burning velocity by adding O_3 is controlled by the close interaction of O_3 decomposition pathways with the distinctive fuel chemistry. Although not shown in the figure, the H abstraction reaction by H atoms was found to be a major route for propane consumption pathways ($\sim 85\%$ at $\phi = 1.0$), whereas its contribution in a stoichiometric methane/air mixture substantially decreased to $\sim 40\%$ ($\sim 47\%$ by OH). This exclusive propane consumption pathway relying on H atoms partially explains the reason why the O_3 decomposition pathway was guided to the reaction (R.1). Considering that all n-alkane chemistries are essentially similar to propane chemistry, comparable enhancement behaviors of n-alkane flames with ozone can be speculated. On the other hand, further investigation of O_3 addition to other hydrocarbons, particularly aromatics, would be a very interesting future study due to the role of O in benzene oxidation pathways [49,50].

4. Concluding remarks

The effects of ozone on the stability characteristics of premixed methane/air and propane/air flames in a nitrogen co-flow were investigated experimentally and interpreted further by chemical kinetic simulations of laminar burning velocities. By adding ozone, flame heights and standoff distances were found to decrease, implying the enhancement of the corresponding laminar burning velocities. Near the rich-flammability-limit of propane/air flames, a nozzle attached polyhedral flame and a spinning partially attached flame were also re-stabilized through the aid of ozone, demonstrating extended flammability limits as well. Significant increases in blowoff velocities were also observed, showing the linear dependence of their percent enhancement on a tested range of ozone concentration in air up to 3810 ppm, regardless of equivalence ratios. The minimum enhancement occurred near-stoichiometric conditions for both fuels, exhibiting the stronger effect of ozone for lean and rich mixtures with 3810 ppm of ozone. As results of the chemical kinetic simulations, the experimentally observed trends of the enhancement in $u_{b,o}$ were predominantly affected by the modification of the laminar burning velocity for a given equivalence ratio. Comprehensive numerical analysis identified that the competition between the two major ozone decomposition pathways, $\text{O}_3 + \text{N}_2 \rightarrow \text{O} + \text{O}_2 + \text{N}_2$ and $\text{O}_3 + \text{H} \rightarrow \text{O}_2 + \text{OH}$,

caused by the interaction with the fuel consumption pathways between methane and propane, was the key mechanism for the enhancement of laminar burning velocity, and consequently blowoff velocity. The ozone decomposition reaction of $\text{O}_3 + \text{N}_2 \rightarrow \text{O} + \text{O}_2 + \text{N}_2$ was found to be the most effective pathway for enhancing the laminar burning velocity, since the reaction of fuel + O provided active OH radicals, which could be used simultaneously for both fuel decomposition and H production. The reaction of $\text{O}_3 + \text{H} \rightarrow \text{O}_2 + \text{OH}$ became more pronounced particularly for near-stoichiometric methane/air flames by the interaction with normal methane oxidation. This resulted in less effective enhancement of the laminar burning velocity by ozone addition for methane/air flames compared to that of propane/air flames for near stoichiometric mixtures.

Acknowledgments

This work was partially supported by the KAUST AEA project.

References

- [1] S.A. Bozhenkov, S.M. Starikovskaia, A.Y. Starikovskii, *Combust. Flame* 133 (1–2) (2003) 133–146.
- [2] G. Lou, A. Bao, M. Nishihara, S. Keshav, Y.G. Utkin, J.W. Rich, W.R. Lempert, I.V. Adamovich, *Proc. Combust. Inst.* 31 (2) (2007) 3327–3334.
- [3] T. Ombrello, Y. Ju, *IEEE Trans. Plasma Sci.* 36 (6) (2008) 2924–2932.
- [4] N.L. Aleksandrov, S.V. Kindysheva, I.N. Kosarev, S.M. Starikovskaia, A.Y. Starikovskii, *Proc. Combust. Inst.* 32 (1) (2009) 205–212.
- [5] T. Nomaguchi, S. Koda, *Symp. (Int.) Combust.* 22 (1) (1989) 1677–1682.
- [6] W. Kim, H. Do, M.G. Mungal, M.A. Cappelli, *IEEE Trans. Plasma Sci.* 34 (6) (2006) 2545–2551.
- [7] W. Kim, H. Do, M.G. Mungal, M.A. Cappelli, *Combust. Flame* 153 (4) (2008) 603–615.
- [8] W. Kim, M.G. Mungal, M.A. Cappelli, *Combust. Flame* 157 (2) (2010) 374–383.
- [9] M.S. Cha, H. Do, M.G. Mungal, M.A. Cappelli, *Combust. Flame* 159 (10) (2012) 3128–3137.
- [10] H. Ohisa, I. Kimura, H. Horisawa, *Combust. Flame* 116 (4) (1999) 653–661.
- [11] M.S. Cha, S.M. Lee, K.T. Kim, S.H. Chung, *Combust. Flame* 141 (4) (2005) 438–447.
- [12] T. Ombrello, S.H. Won, Y. Ju, S. Williams, *Combust. Flame* 157 (10) (2010) 1906–1915.
- [13] T. Ombrello, S.H. Won, Y. Ju, S. Williams, *Combust. Flame* 157 (10) (2010) 1916–1928.
- [14] W. Sun, M. Uddi, S.H. Won, T. Ombrello, C. Carter, Y. Ju, *Combust. Flame* 159 (1) (2012) 221–229.
- [15] M.K. Kim, S.H. Chung, H.H. Kim, *Combust. Flame* 159 (3) (2012) 1151–1159.
- [16] A.Y. Starikovskii, *Proc. Combust. Inst.* 30 (2) (2005) 2405–2417.
- [17] S.H. Won, M.S. Cha, C.S. Park, S.H. Chung, *Proc. Combust. Inst.* 31 (1) (2007) 963–970.
- [18] K. Takita, *Combust. Flame* 128 (3) (2002) 301–313.
- [19] K. Takita, A. Moriwaki, T. Kitagawa, G. Masuya, *Combust. Flame* 132 (4) (2003) 679–689.
- [20] K. Takita, N. Abe, G. Masuya, Y. Ju, *Proc. Combust. Inst.* 31 (2) (2007) 2489–2496.
- [21] I. Kimura, H. Aoki, M. Kato, *Combust. Flame* 42 (1981) 297–305.
- [22] M. Uddi, N. Jiang, E. Mintusov, I.V. Adamovich, W.R. Lempert, *Proc. Combust. Inst.* 32 (1) (2009) 929–936.
- [23] M.K. Kim, S.K. Ryu, S.H. Won, S.H. Chung, *Combust. Flame* 157 (1) (2010) 17–24.
- [24] S.M. Lee, C.S. Park, M.S. Cha, S.H. Chung, *IEEE Trans. Plasma Sci.* 33 (5) (2005) 1703–1709.
- [25] M.K. Kim, S.H. Chung, H.H. Kim, *Proc. Combust. Inst.* 33 (1) (2011) 1137–1144.
- [26] S.H. Won, S.K. Ryu, M.K. Kim, M.S. Cha, S.H. Chung, *Combust. Flame* 152 (4) (2008) 496–506.
- [27] M.S. Cha, Y. Lee, *IEEE Trans. Plasma Sci.* 40 (12) (2012) 3131–3138.
- [28] D.H. Lee, K.-T. Kim, M.S. Cha, Y.-H. Song, *Proc. Combust. Inst.* 31 (2) (2007) 3343–3351.
- [29] D.H. Lee, K.-T. Kim, M.S. Cha, Y.-H. Song, *Int. J. Hydrogen Energy* 35 (10) (2010) 4668–4675.
- [30] M.S. Cha, Y.-H. Song, J.-O. Lee, S.J. Kim, *Int. J. Plasma Environ. Sci. Tech.* 1 (1) (2007) 28–33.
- [31] F. Foucher, P. Higelin, C. Mounaïm-Rousselle, P. Dagaut, *Proc. Combust. Inst.* 34 (2) (2013) 3005–3012.
- [32] Z.H. Wang, L. Yang, B. Li, Z.S. Li, Z.W. Sun, M. Aldén, K.F. Cen, A.A. Konnov, *Combust. Flame* 159 (1) (2012) 120–129.
- [33] F. Halter, P. Higelin, P. Dagaut, *Energy Fuels* 25 (7) (2011) 2909–2916.
- [34] T. Tachibana, K. Hirata, H. Nishida, H. Osada, *Combust. Flame* 85 (3–4) (1991) 515–519.
- [35] H. Nishiyama, H. Takana, S. Niikura, H. Shimizu, D. Furukawa, T. Nakajima, K. Katagiri, Y. Nakano, *IEEE Trans. Plasma Sci.* 36 (4) (2008) 1328–1329.

- [36] Y. Matsubara, K. Takita, G. Masuya, Proc. Combust. Inst. 34 (2) (2013) 3287–3294.
- [37] F.M. White, Fluid Mechanics, fourth ed., McGraw-Hill, New York, 1998. p. 331.
- [38] R. Morrissey, C. Schubert, Combust. Flame 7 (3) (1963) 263–268.
- [39] K.K. Kuo, Principles of Combustion, second ed., John Wiley & Sons, New Jersey, 2005. p. 439.
- [40] C.K. Law, D.L. Zhu, G. Yu, Symp. (Int.) Combust. 21 (1) (1988) 1419–1426.
- [41] C.M. Vagelopoulos, F.N. Egolfopoulos, Symp. (Int.) Combust. 27 (1) (1998) 513–519.
- [42] B. Lewis, G. von Elbe, Combustion, Flames and Explosions of Gases, second ed., Academic Press, Florida, 1961.
- [43] S.H. Won, W. Sun, Y. Ju, Combust. Flame 157 (3) (2010) 411–420.
- [44] S.H. Won, S. Dooley, F.L. Dryer, Y. Ju, Combust. Flame 159 (2) (2012) 541–551.
- [45] H.H. Kim, S.H. Won, J. Santner, Z. Chen, Y. Ju, Proc. Combust. Inst. 34 (1) (2013) 929–936.
- [46] M.J. Kwon, B.J. Lee, S.H. Chung, Combust. Flame 105 (1–2) (1996) 180–188.
- [47] CHEMKIN-PRO Package, Reaction Design, 6440 Lusk Boulevard, Suite D-205 San Diego, CA 92121. <<http://www.reactiondesign.com>>.
- [48] H. Wang, X. You, A.V. Joshi, S.G. Davis, A. Laskin, F. Egolfopoulos, C.K. Law, High Temperature Combustion Reaction Model of H₂/CO/C₁–C₄ Compounds, May 2007. <http://ignis.usc.edu/USC_Mech_II.htm>.
- [49] S.G. Davis, H. Wang, K. Breinsky, C.K. Law, Symp. (Int.) Combust. 26 (1) (1996) 1025–1033.
- [50] R.P. Lindstedt, G. Skevis, Combust. Flame 99 (3–4) (1994) 551–561.